www.ijprems.com
editor@ijprems.com

INTERNATIONAL JOURNAL OF PROGRESSIVE RESEARCH IN ENGINEERING MANAGEMENT AND SCIENCE (IJPREMS)

Vol. 03, Issue 08, August 2023, pp : 322-328

e-ISSN : 2583-1062

Impact Factor : 5.725

AN APPROACH TO DISTRIBUTED AND GENERATION AND VIRTUAL STATCOM SYSTEM AND CONTROL

Dr. N. Sambasiva Rao[1], A. Tanuja[2], Mr. K. Venkata Kishore[3], Ch. Veera Murali Krishna[4], P. Leela Supriya[5], Durga prasad[6], P. Aakash[7]

[1]Professor and Head of the Department of Electrical and Electronics Engineering (EEE). NRI Institute of Technology (Autonomous), Vijayawada, India.

[2,4,5,6,7]Department of Electrical and Electronics Engineering (EEE). NRI Institute of Technology (Autonomous), Vijayawada, India.

[3]Associate Professor of the Department of Electrical and Electronics Engineering (EEE). NRI Institute of Technology (Autonomous), Vijayawada, India.

DOI : https://www.doi.org/10.56726/IRJMETS31952

ABSTRACT

As DG connections grow, distribution system voltage stability is threatened. Reactive power compensators like static synchronous compensators (STATCOM) can handle voltage stability degradation. STATCOM's complex distribution architecture makes placement difficult. If installed at the wrong place, economic efficiency and availability may suffer. This study proposes Virtual STATCOM Configuration and Control to make several DGs act as a single STATCOM. The proposed Virtual STATCOM uses existing facilities without constructing new power facilities, making it cost-effective and solves the problem of the distribution system's complexity making it hard to identify an installation location. The Virtual STATCOM controls numerous DGs attached to the system to alter the Point of Common Coupling (PCC) power quality, whereas the standard STATCOM controls the access point's power quality separately. Linear programming is used to configure the Virtual STATCOM integrated control algorithm to compensate for distance between the DG and PCC, inverter capacity, and power generation.

Keywords: Static Compensator STATCOM, Point of common coupling (PCC), Distributed Generation DG

1. INTRODUCTION

To deal with the massive growth in electrical energy consumption and to lessen environmental issues caused by the usage of fossil fuels, the integration of RESs into electrical networks has become a required and crucial topic. Wind, PV, fuel cells, and biomass are just a few examples of RES that are put to use in the electric power industry. The yearly growth rate of RES, Fig. 1, shows that wind and PV are the two most integrated RES into electricity systems due to their many benefits [1-2].

In instances of fault events, hybrid power systems that are dependent on wind energy conversion systems (WECSs) and photovoltaic (PV) systems are unable to provide the required reactive power. Consequently, fluctuations in the voltage profile will occur at the point of common coupling (PCC) when the renewable energy sources (RES) are interconnected with the electrical grid [3-6]. Voltage spikes and dips have a detrimental effect on the dependability, efficiency, and quality of the power system.Certain grid codes, such as the Nordal grid code illustrated in Figure 2, specify that failure to effectively regulate voltage fluctuations can lead to undesirable magnitudes, causing the disconnection of renewable energy sources (RESs) from the system due to their inability to provide sufficient reactive power support during these faults.

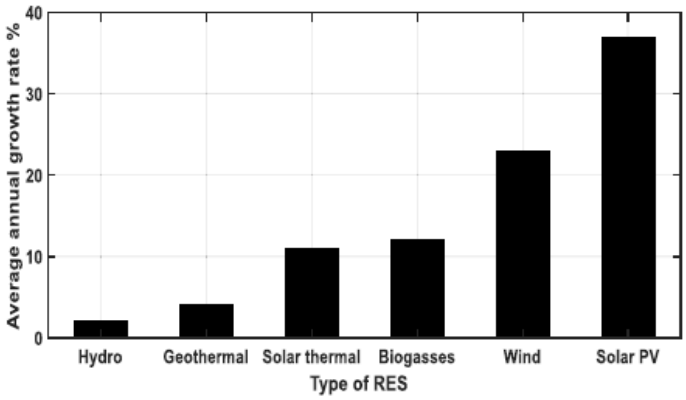

Fig 1 Annual growth rate of some RESs.

INTERNATIONAL JOURNAL OF PROGRESSIVE RESEARCH IN ENGINEERING MANAGEMENT AND SCIENCE (IJPREMS)

www.ijprems.com
editor@ijprems.com

Vol. 03, Issue 08, August 2023, pp : 322-328

e-ISSN : 2583-1062

Impact Factor : 5.725

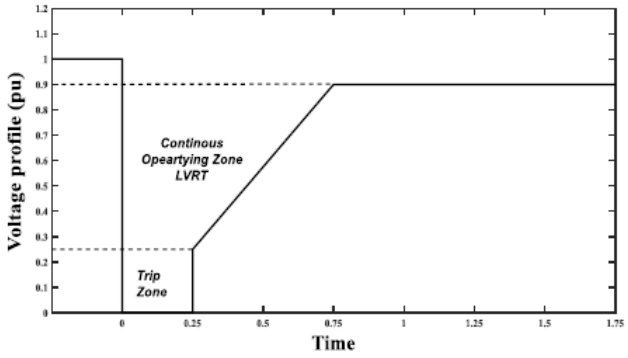

Fig 2 Nordal grid code.

Some grid rules stipulate that RESs must be disconnected from the system if voltage fluctuations are not controlled properly, since the absence of support for the system's reactive power during these failures causes the RESs to fail.

2. STATCOM PRINCIPLE OF OPERATION AND CONTROL

The PCC voltage is used to regulate the static shunt compensator, or STATCOM, which produces a capacitive/inductive output current. STATCOM's single-line diagram and control block diagram help explain how the system works . The primary components of STATCOM are a voltage source converter (VSC), a DC capacitive energy storage device, and a coupling transformer that shunts the VSC into the PCC power grid [9]. The VSC creates a range of variable voltages at the frequency of the alternating current power grid. By adjusting the reference voltage to 1pu from a 0.26 kV base voltage, STATCOM may switch between capacitive and inductive modes of operation. If the PCC voltage amplitude drops, the STATCOM will create reactive power (capacitive mode) by injecting a leading current into the grid at PCC. In the inductive mode, STATCOM injects a lagging current into the grid at PCC. When the PCC rises, the reactive power is taken up by the STATCOM [11].

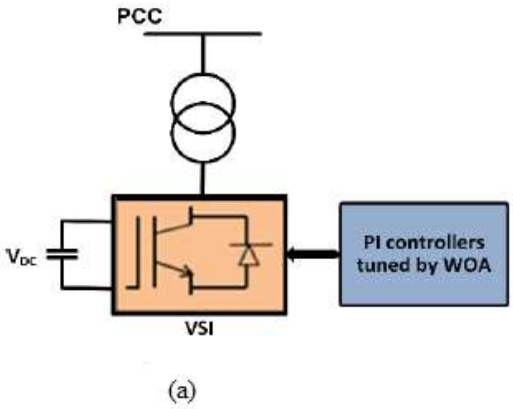

Fig 3 STATCOM circuit representation. (a) Single-phase diagram of

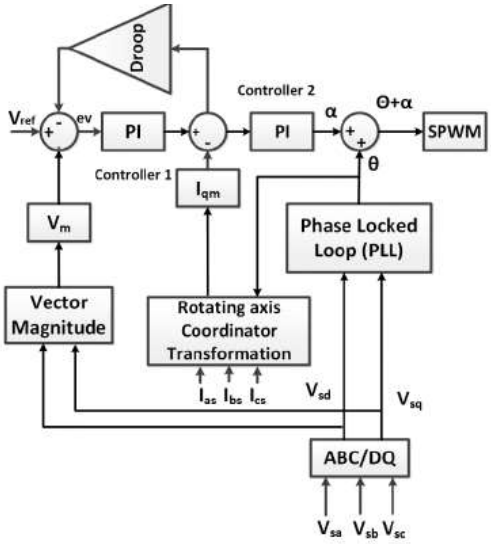

Fig 4 STATCOM circuit representation.

www.ijprems.com
editor@ijprems.com

INTERNATIONAL JOURNAL OF PROGRESSIVE RESEARCH IN ENGINEERING MANAGEMENT AND SCIENCE (IJPREMS)

Vol. 03, Issue 08, August 2023, pp : 322-328

e-ISSN : 2583-1062

Impact Factor : 5.725

No power is sent until the PCC voltage is altered. The STATCOM-injected current may be adjusted to reduce PCC voltage oscillations during fault conditions. The primary contribution of this study is the near-optimal scheduling of two PI controllers to effectively drive the STATCOM to reduce voltage fluctuations and enhance the dynamic performance of the hybrid system. Parameters for both PI controllers are scheduled [7]. Voltage and current are illustrated in Fig. 2., together with the STATCOM block diagram and the two optimised PI controllers. The two suggested controllers are mostly used for STATCOM operation. Based on the discrepancy between the measured and reference voltage signals, Controller 1 is assumed to properly update the quadrature-axis current reference, Iqref . The phase angle of the PCC terminal voltage, represented by, is primarily controlled by Controller 2. This study presents the Synchronous Pulse Width Modulation (SPWM) approach for generating the switching pulses of the STATCO's three-level inverter. In this way, the phase angle _ control regulates the grid-supplied power from the inverter. This paper's main contribution is a set of near-optimal settings for the PI controller used in STATCOM. The dynamic performance of the system under control of the two optimised PI controllers is compared and contrasted in an objective manner using PSO, an alternative optimisation approach.

3. DESIGN CONTROLLERS

a. PI CONTROLLERS

It is a compound control mode obtains by combine proportional and integral mode. The geometric expression for such a merged control is,

$$m(t) = K_p\, e(t) + K_i \int e(t)$$

here preliminary rate of the output at +=0 The significant benefit of this control is that one to one association of proportional mode is obtainable with the offset gets eliminate due to integral mode, the integral part of such a combined control provides a reset of the zero errors output after a load change occurs. Consider the load change happening at t=t1t1 and due to which error values

b. Model predictive controller

The major intent of the control approach is to estimate the inverter output voltage, uI, abc, to control the dc-link output to the reference voltage of the capacitor, V*, dc to the load and infused into the smart grid voltage and current command reference, Q*. There are numerous alternatives for scheming the control algorithm for an AFE. In general, a parallel control scheme is used. An peripheral control loop is engaged to control the dc link voltage. Alternatively, an inner control loop is adopted to follow the smart grid voltage and current references concerning the transfer function applied to expand this MP controller. The block--diagram of model predictive controller (MPC)' is appeared in Fig 5. In model predictive controller, the most of the controller comprise inaccuracy of double or numerous states of the-system in the Plant-surface Example grid side load-current, voltage and DC Link voltage.

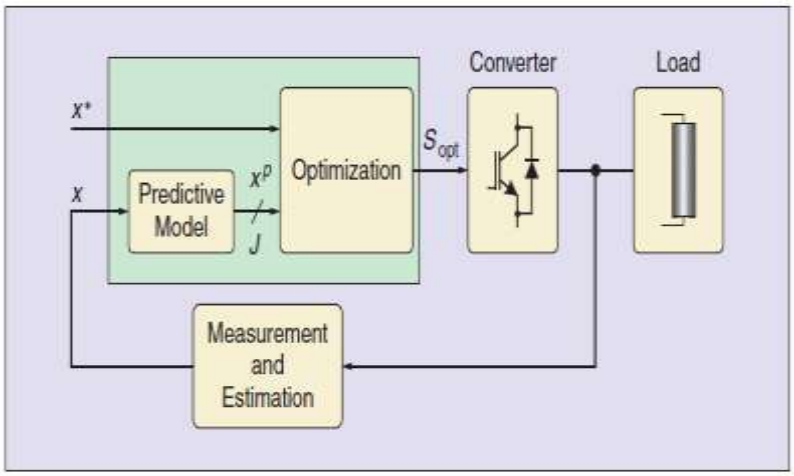

Fig 5 Block-Diagram of model predictive controller

additionally, different -controller comprises error &both of the time-derivatives and the -integral of the-error in the MPC –optimization to control time domain response of the-system. In this-case, the MPC-plant converter can be control as a voltage and current which broad mathematical revision is appreciative to guarantee-system-steadiness. Another plant converter is painstaking in for the improvement in the steady-state-error& settling-time, which comprises voltage-error & grid side load current.

www.ijprems.com
editor@ijprems.com

INTERNATIONAL JOURNAL OF PROGRESSIVE RESEARCH IN ENGINEERING MANAGEMENT AND SCIENCE (IJPREMS)

Vol. 03, Issue 08, August 2023, pp : 322-328

e-ISSN : 2583-1062

Impact Factor : 5.725

4. RESULTS AND DISCUSSION

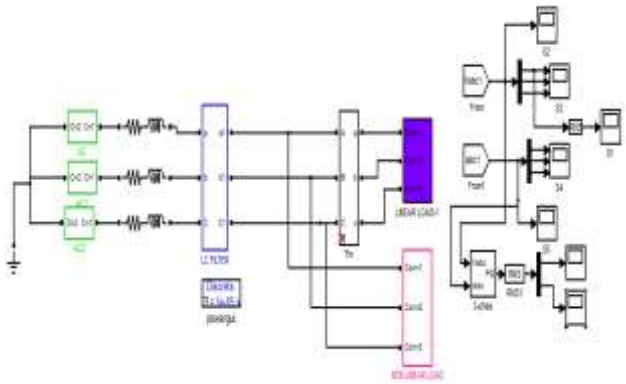

Fig 6 Circuit diagram of without STATCOM

Figure 6 displays the circuit design in the absence of a Static Synchronous Compensator (STATCOM). This illustrates the output voltage, which has a magnitude of 170V.

The 415V output may be shown in fig. 3.21. Figure 3.22 displays the THD percentage for the output voltage, which is 5.41%. The 2.1A output current is shown in fig. 3.23. Fig. 3.24 displays the Total Harmonic Distortion (THD) of the output current. Figure 3.25 displays the actual power output, which is 1180W. Figure 3.26 displays the 950VAR value of reactive power.

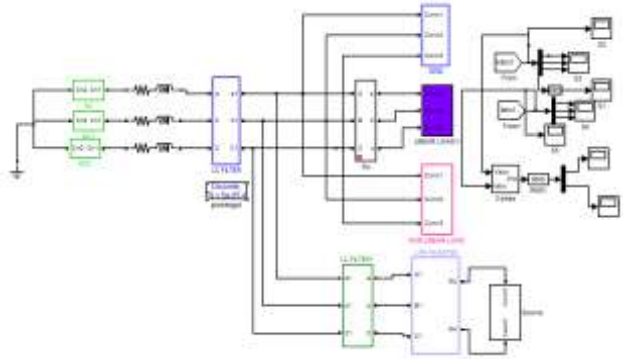

Fig 7 Circuit diagram of with STATCOM

The circuit design depicting the inclusion of a Static Synchronous Compensator (STATCOM) is seen in Figure 6. The voltage across the RL load. The figure 15 illustrates the Total Harmonic Distortion (THD) of the output voltage, with a measured value of 6.82%. The figure shown in Figure 16 illustrates the current flowing through the RL load, with a magnitude of 1.8A. It illustrates the current total harmonic distortion (THD) and indicates that its magnitude is 5.04%. The graphical representation of power, as seen in Figure 10, exhibits a value of 640W. The figure 19 illustrates the representation of reactive power, with a magnitude of 500 VAR.

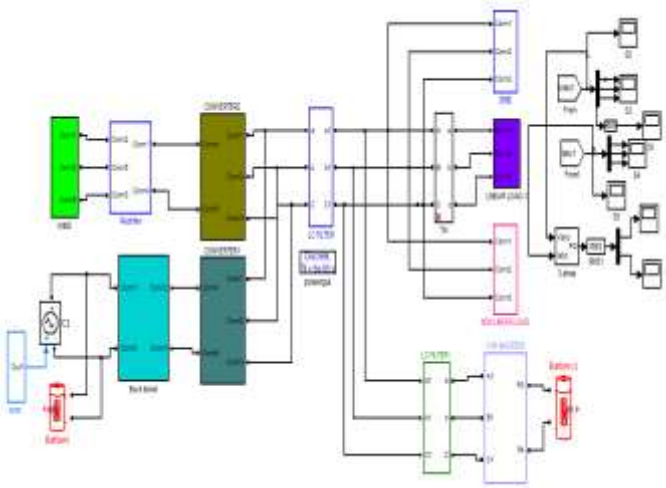

Fig 8 Circuit diagram of with E-STATCOM

www.ijprems.com
editor@ijprems.com

INTERNATIONAL JOURNAL OF PROGRESSIVE RESEARCH IN ENGINEERING MANAGEMENT AND SCIENCE (IJPREMS)

Vol. 03, Issue 08, August 2023, pp : 322-328

e-ISSN : 2583-1062

Impact Factor : 5.725

Circuit diagram of with E-STATCOM is shown in fig 8. Circuit diagram of buck boost converter is shown in fig 3.17. Switching pulse of buck boost converter M1 &M2 is shown in fig 3.18 and its value is 1V. Voltage across buck boost converter is shown in fig 3.19 and its value is 90V. Switching pulse of three phase inverter M1, M3 and M5 is shown in fig 3.20 and its value is 1V.

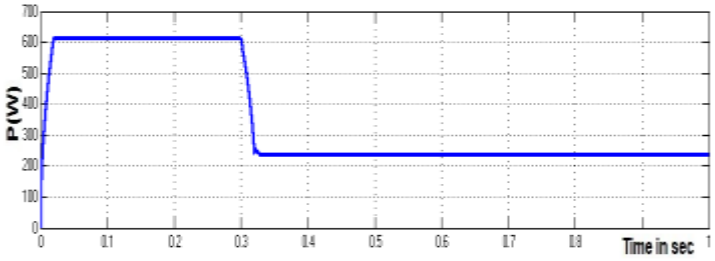

Fig 9 Real power

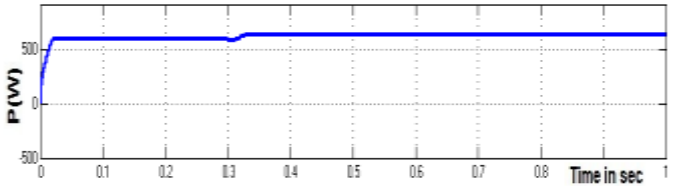

Fig 10 Real power

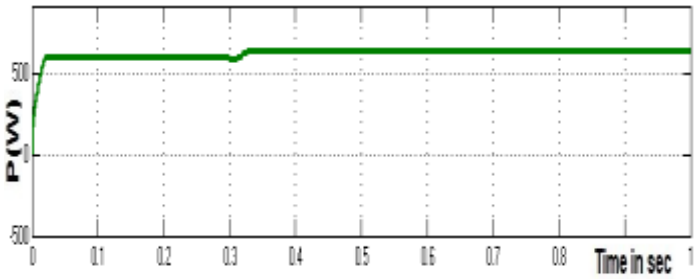

Fig 11 Reactive Power

Table 1 Comparison output voltage, Real & Reactive Power

STATCOM	Vo(V)	P(W)	Q(VAR)
Without STATCOM	170	240	180
With STATCOM	300	640	500
With E- STATCOM	415	1180	950

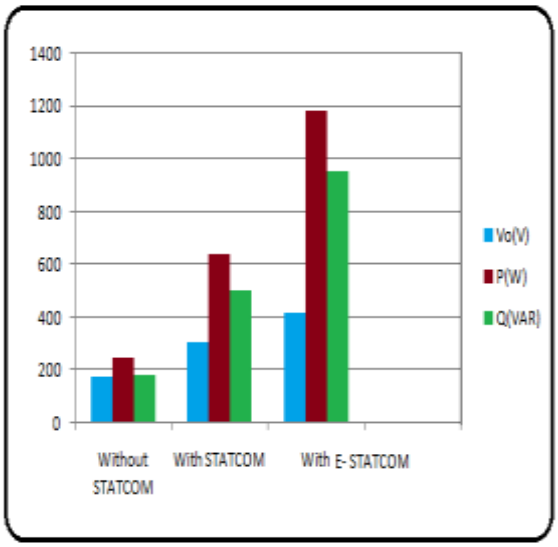

Fig 12 Bar chart comparison of output voltage, Real & Reactive Power

www.ijprems.com
editor@ijprems.com

INTERNATIONAL JOURNAL OF PROGRESSIVE RESEARCH IN ENGINEERING MANAGEMENT AND SCIENCE (IJPREMS)

Vol. 03, Issue 08, August 2023, pp : 322-328

e-ISSN : 2583-1062

Impact Factor : 5.725

Table 2 Comparison output voltage THD and output current THD

DVR	Voltage THD (%)	Current THD (%)
Without STATCOM	19.56	17.95
With STATCOM	6.82	5.04
With E- STATCOM	5.41	4.87

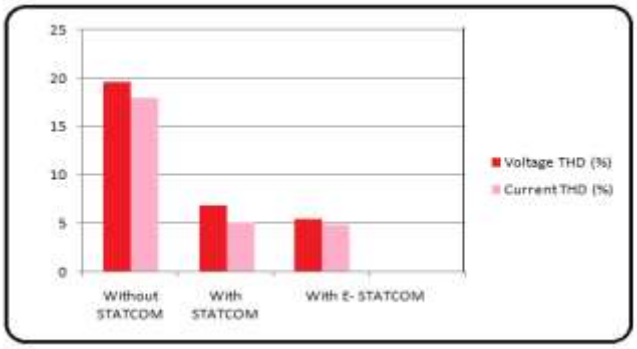

Fig 13 Bar chart comparison of output voltage THD and output current THD

Table 1 presents a comparative analysis of the existing system and the proposed system, focusing on their respective output voltage, real power, and reactive power. Figure 32 presents a bar chart that compares the voltage, real power, and reactive power outputs of the existing and planned systems. Table 2 presents a comparative analysis of the total harmonic distortion (THD) of the output voltage and current for both the existing system and the proposed system. The bar chart in Figure 13 illustrates the total harmonic distortion (THD) of the output voltage and output current of the system under consideration.

5. CONCLUSION

The simulation employs a circuit design of a system without a STATCOM component. A circuit diagram simulation of the STATCOM system is conducted. A circuit diagram simulation of the E-STATCOM system is conducted. The approaches listed above are being compared. The use of the E-STATCOM system leads to a substantial rise in the output voltage, elevating it from 170V to 415V. The use of E-STATCOM technology enables a significant increase in effective power, elevating it from 240 W to 1180 W. The implementation of the E-STATCOM system leads to a significant augmentation in the reactive power level, which escalates from 180VAR to 950VAR. By implementing the E-STATCOM system, a significant reduction in the total harmonic distortion (THD) of the output voltage was achieved, decreasing it from 19.56% to 5.41% V. The use of E-STATCOM technology has the potential to significantly reduce the total harmonic distortion (THD) of the output current, decreasing it from 17.95% to 4.87%. Consequently, the E-STATCOM system exhibits a higher level of performance compared to the regular STATCOM system.The removal of these Renewable Energy Sources (RESs) from the system is attributed to their failure in providing enough support for the system's reactive power during these disturbances.

6. REFERENCES

[1] N. G. Hingorani and L. Gyugyi, Understanding Facts: Concept and Technology of Flexible AC Transmission Systems. Piscataway, NJ, USA: IEEE Press, 2000.

[2] L.Gyugyi, C.D. Schauder, S. L. Williams, T. R. Rietman, D. R. Torgerson, andA. Edris, “The unified power flowcontroller: Anewapproach to power transmission control,” IEEE Trans. Power Del., vol. 10, no. 2, pp. 1085–1097, Apr. 1995.

[3] A. Rajabi-Ghahnavieh, M. Fotuhi-Firuzabad, M. Shahidehpour, and R. Feuillet, “UPFC for enhancing power system reliability,” IEEE Trans.Power Del., vol. 25, no. 4, pp. 2881–2890, Oct. 2010.

[4] H. Fujita, Y. Watanabe, and H. Akagi, “Control and analysis of a unified power flow controller,” IEEE Trans. Power Electron., vol. 14, no. 6,pp. 1021–1027, Nov. 1999.

[5] M. A. Sayed and T. Takeshita, “Line loss minimization in isolated substations and multiple loop distribution systems using the UPFC,” IEEE Trans. Power Electron., vol. 29, no. 11, pp. 5813–5822, Jul. 2014.

[6] H. Fujita, Y. Watanable, and H. Akagi, “Transient analysis of a unified power flow controller and its application to design of dc-link capacitor,” IEEE Trans. Power Electron., vol. 16, no. 5, pp. 735–740, Sep. 2001.